IV International Conference on Simulation for Additive Manufacturing
Sim-AM 2023
E. Rank and S. Kollmannsberger (Eds)

THE EFFECT OF GEOMETRICAL IMPERFECTIONS ON THE MECHANICAL PROPERTIES OF LATTICE STRUCTURES PRODUCED BY THE POWDER BED FUSION (PBF) PROCESS

KOHEI HAMASAKI* **AND KUNIHARU USHIJIMA†**

*Graduate School of Engineering, Tokyo University of Science
6-3-1 Niijyuku, Katushika-ku, Tokyo 125-8585, Japan
e-mail: 4522540@ed.tus.ac.jp/

†Faculty of Engineering, Tokyo University of Science
6-3-1 Niijyuku, Katushika-ku, Tokyo 125-8585, Japan
e-mail: kuniharu@rs.tus.ac.jp

Key words: 3D Printing, Additive manufacturing, Compression test, Finite Element Method, Geometrical imperfection, Lattice structures

Abstract. In this paper, the effects of geometrical imperfections observed in a lattice structure fabricated by metal 3D printer on the compressive response were investigated by using FE simulation. Geometrical imperfections which are due to excessive heat transfer and the melting of unnecessary metal powder during the fabrication process was observed using a 3D X-Ray microscope (XRM) machine. Based on the observation, two types of geometrical imperfections (strut diameter deviation and the center-axis offset) were measured, and the quantities of these imperfections on the mechanical properties of lattice block were discussed. By introducing imperfections to the FE model, a likelihood of reduced mechanical properties can be potentially adverted. In addition, by comparing the amount of geometrical imperfections, the initial stiffness and plastic collapse strength in the models based on different strut diameters, we proposed appropriate manufacturing conditions for the lattice blocks that would minimize the reduction of their mechanical properties.

1 INTRODUCTION

In recent years, due to the rapid development in additive manufacturing (AM) technology, such as metal 3D printers, have made it possible to create more precise and more complex shapes that were difficult to create by the conventional manufacturing technology [1, 2]. While the creation of molds is required when a structure is manufactured by castings, AM technologies, such as selective laser sintering (SLS) or electron beam melting (EBM) can produce it easily by preparing CAD data only. This is advantageous in terms of time and cost, as well as in terms of environmental impact, especially for manufacturing one-off items. In the future, it is expected to play an active role in a wide range of industrial fields, such as automotive and aerospace parts, and medical fields, such as implants. To date, various studies have been conducted for the mechanical properties of porous structures fabricated by metal 3D printers [3, 4, 5, 6, 7]. According to many reports, it is widely known that the mechanical properties vary depending

on the melting conditions, and the measured values are much lower than the theoretical values as designed. This fact has been identified as an important issue in AM technology. One of the reasons for such problem is that when heat is applied to metal powders via a laser beam during fabrication, excessive heat melts unnecessary powders, resulting in geometrical imperfections. For example, Pavel et al.[3] summarized the influence of process parameters, such as laser power, scan speed, thickness of layer, overlap rate and building direction on tensile properties and structure of printing materials. They concluded that the SLS built steel samples usually have better tensile properties than those conventionally manufactured. Also, Cao et al.[4] investigated the mechanical responses of lattice structures with stochastic geometric defects based on the quasi-static compression test. The lattice structures investigated were fabricated by AM technology, and X-ray computed tomography was employed to capture the morphology and distribution of process-induced defects, such as strut porosity, strut thickness variation and strut waviness, in order to clarify their role in the elastic response, damage initiation and failure evolution. On the other hand, Gumruk et al.[5] reported the mechanical static compression behavior of 316L stainless steel micro-lattice materials manufactured using selective laser melting method. In their study, the material overlapping effects in the vicinity of strut connection points was taken into consideration to give reasonable predictions corresponding to the initial stiffness and strength values of the lattices. Also, Liu et al.[6] measured the amount of geometrical imperfections of beams in octet lattice and orthorhombic cubic octahedron structures, and reported that this value differs between vertically and horizontally printed beams. Moreover, Lozanovski et al.[7] proposed a method of generating CAD AM representative strut model and concluded that this model shows greater correlation toward experiment and more realistic deformation behaviors. As described above, the magnitude of geometrical imperfections that occur during AM and their effects on mechanical properties are still being investigated for a variety of shapes, materials, and fabricating conditions. In this study, the effects of observed geometrical imperfection on the mechanical properties of SUS630 lattice blocks fabricated by SLS technique. During observation, geometrical imperfections are considered to be roughly classified into two categories: radial misalignment and eccentricity of the central axis. The main motivation of this study is to clarify the main factors that contribute to the reduction of mechanical properties. In addition, by comparing the amount of geometrical imperfections and mechanical properties for models with different strut diameters, we will propose not only an appropriate productive condition for the lattice block but also an estimation method for the initial stiffness and plastic collapse strength for the lattice structures.

2 EXPERIMENTAL INVESTIGATION AND NUMERICAL SIMULATION

2.1 Fabrication of Lattice Block

The BCC micro-lattice specimens shown in Figure 1(a,b) were manufactured by using our in-house metal 3D printer (ProX 300, 3D Systems Ltd.). The material was made of gas-atomized SUS630 powder, and the median diameter of a sphere was around 20 µm. The manufacturing process parameters were shown in Table 1. Also, the definitions of these parameters were found in Figure 2.

Based on these manufacturing parameters shown in Table 1, a lattice cube with 30 mm on each side was fabricated. This lattice is consisted of BCC unit cells with a strut length $L = 3.75$ mm and a strut diameter $d = 0.3$ mm unless otherwise specified.

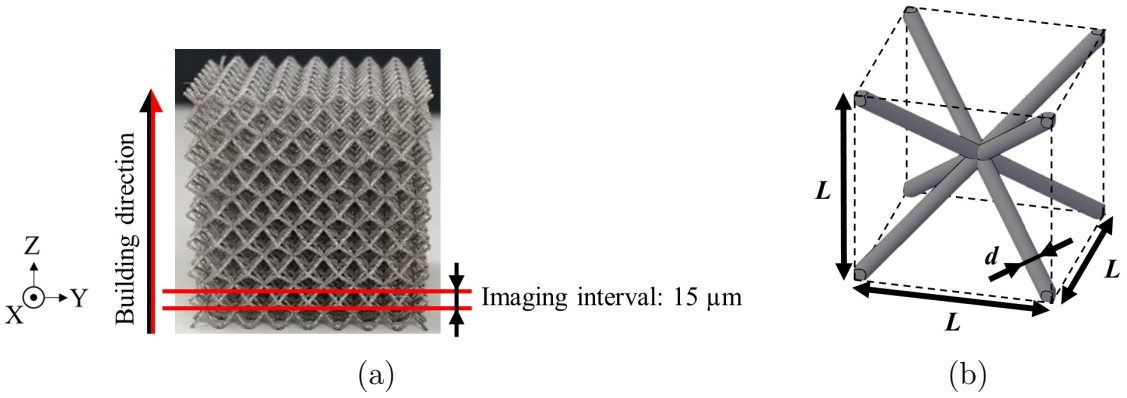

Figure 1: BCC lattice structure fabricated by metal 3D printer and the definition of unit-cell geometries

Table 1: Manufacturing conditions in a metal 3D printer

Laser style	Normal
Laser power p [W]	150
Laser pitch d_p [µm]	20
Layer thickness t_i [µm]	40
Scanning speed ν [mm/s]	1000

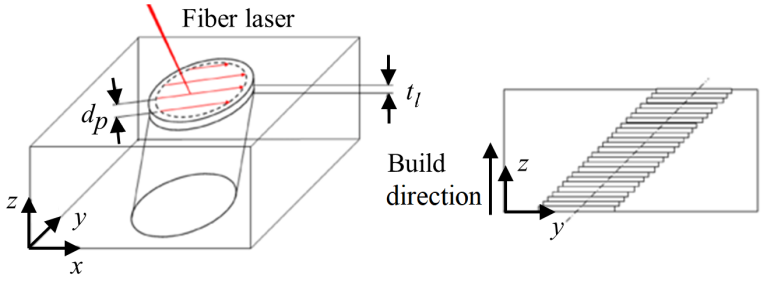

Figure 2: Definition of manufacturing parameters for a strut

2.2 Geometrical Defects Investigation

In order to measure the geometrical imperfections, a 3D X-Ray microscope (XRM) machine (SKYSCAN 2214, Bruker) was used for the specimen. Four cells located in the center of a cube were captured in the same direction along the building direction. Here, the imaging interval was set to 15 µm.

The observed XRM images were binarized by using an image processing software, Image J. Figure 3(a) shows an example of binarized XRM image. Every strut in a lattice core has designed as a straight rod with a constant diameter d. The cross-section of the inclined struts scanned by XRM machine becomes elliptical. In addition, during fabrication, an excessive heat travels to the backyard of the struts, the cross-section of the manufactured strand differs

significantly from that of the designed one. Based on this fact, in our study, the cross-section of the strut is approximated to an elliptic shape, and measured the imperfections the following parameters were measured from actual XRM image data.

(1) Major and Minor diameter, a and b

(2) Position of the center of the elliptical cross-section, X_c' and Y_c'

The definition of each parameter can be found in Figure 3(b) and (c).

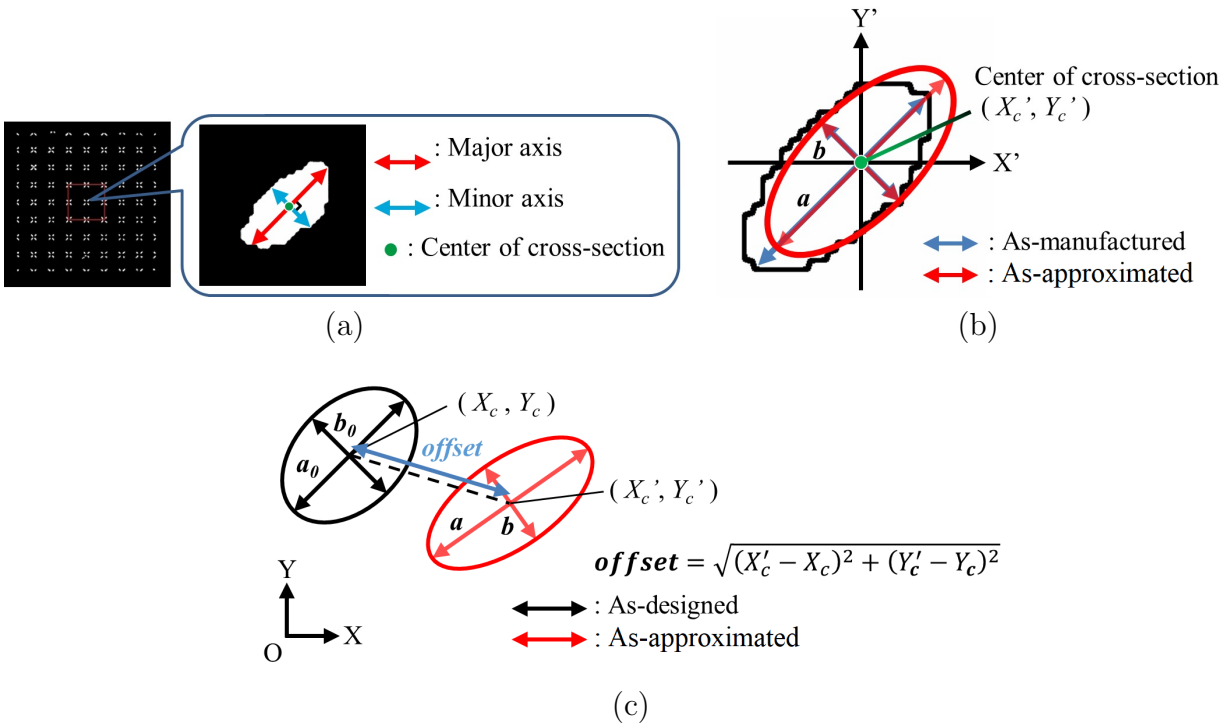

Figure 3: Definition of cross-section information

2.3 Finite Element Analysis Considering Geometrical Imperfections

2.3.1 Analysis Model Based on Investigation

Similar to Lozanovski et al.'s procedure[7], a representative AM model was created by considering the observed geometrical imperfection, and numerical analysis described later was conducted. During our FE simulation, a commercial FE software, MSC.Marc 2022 was used. The quadratic tetrahedral element was selected, and the influence of the radius deviation and center-axis offset on the mechanical properties were confirmed (see Figure 4).

2.3.2 Compression Analysis

A Compression analysis was conducted by using FE simulation for 3D lattice block model. This model includes the observed geometrical imperfections.

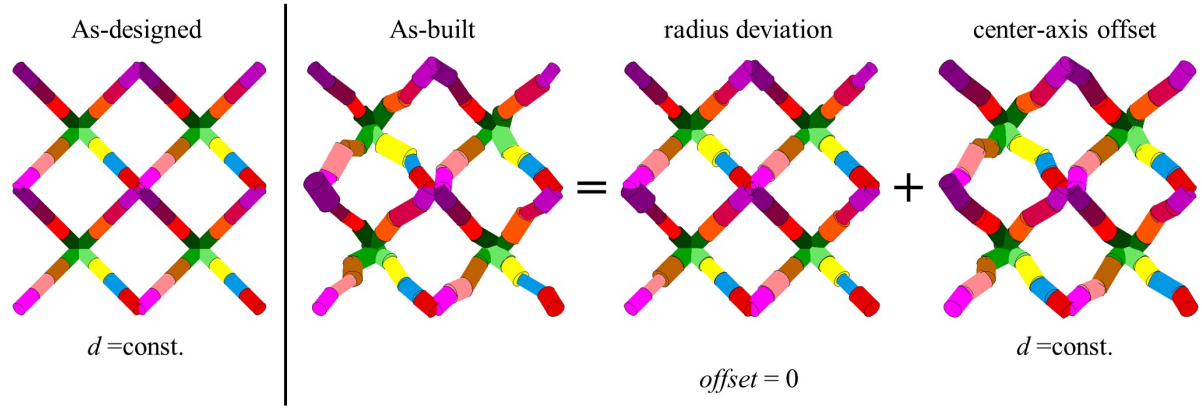

Figure 4: FE model reflecting radius deviation and center-axis offset

Figure 5(a) shows a schematic of boundary condition applied in our FE model. The top rigid surface was moved downward quasi-statically and touched to the FE model. The lower end of the block was fixed to a bottom rigid surface, and the equivalent initial stiffness E^* and the plastic collapse strength σ_y^* were calculated from the load versus displacement relationship for a block model.

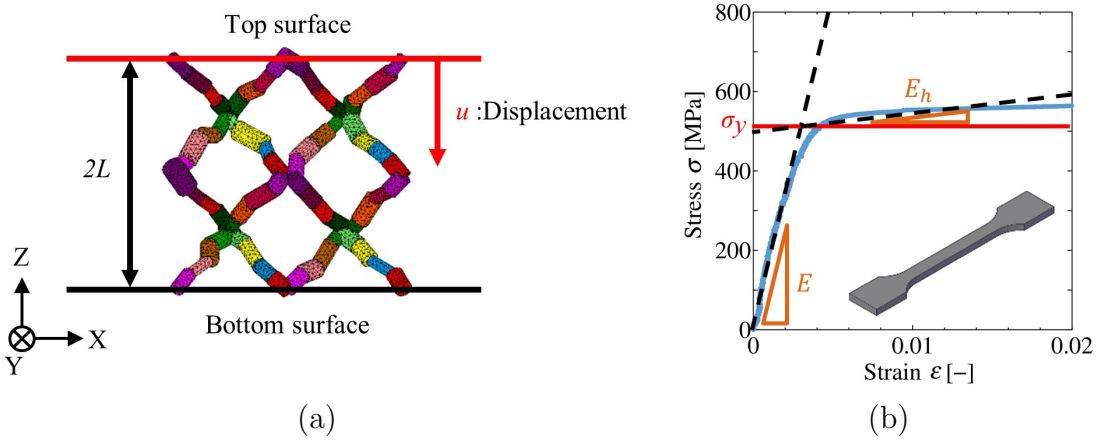

Figure 5: Schematic of compression test for a FE model and stress-strain curve for a tensile specimen

Figure 5(b) shows the measured stress-strain curve for a SUS630 tensile specimen fabricated by our in-house metal 3D printer. In our simulation, the material property is assumed to be homogeneous, isotropic elastoplastic response, and the stress-strain curve is given by the following relationship:

$$\sigma = \sigma_y + \frac{EE_h}{(E - E_h)}\epsilon_p \tag{1}$$

where, σ_y and ϵ_p depict the yield stress and equivalent plastic strain, and E and E_h are the Young's modulus and strain hardening coefficient, respectively. The values of parameters σ_y, E and E_h can be derived from the curve-fitting operation based on the least quare method, and shown in Table 2.

Table 2: Values of material parameters

Young's modulus E [GPa]	191.3
Poisson's ratio ν [-]	0.3
Yield stress σ_y [MPa]	523
Strain hardening coefficient E_h [MPa]	823

2.3.3 Influence of Geometrical Imperfections on E^* and σ_y^*

In order to discuss the influence of observed geometrical imperfections, radius variation and the center-axis offset in a strut on the mechanical response quantitatively, the numerical results obtained from the following four kinds of FE models were compared with the experimental result for a lattice block.

- imperfection-free model which can be regarded as an "as-designed" model
- radius deviation model (See Figure 4 "radius deviation")
- center-axis offset model (See Figure 4 "center-axis offset")
- unified imperfection model (See Figure 4 "As-built")

Regarding the as-designed model, the predictions for the initial stiffness E^* and the plastic collapse strength σ_y^* have been proposed by Gumruk and Mines [5], and given by the following equations:

$$E^* = \frac{9\pi \left(\frac{d}{L}\right)^4 E}{16 \left\{ \left(\frac{\sqrt{3}}{2}\right) - \left(\frac{d}{L}\right) \right\}^3} \qquad (2)$$

$$\sigma_y^* = \frac{4\sqrt{6}\beta \left(\frac{d}{L}\right)^3 \sigma_y^*}{\left(\frac{\sqrt{3}}{2}\right) - \left(\frac{d}{L}\right)}$$

Here, the parameter β shown in Eq.(2) represents a factor and will be determined by reflecting the experimental compression tests of lattice blocks. In this study, β was set to 0.181. Also, in the unified imperfection model, the imperfections of the radius deviation as well as the centre-axis offset were included simultaneously.

The degradation rates of the initial stiffness E^* and the plastic collapse strength σ_y^* were determined from the relative errors among them by comparing FE results for the as-designed model with those with imperfections.

2.4 Effect of Strut Diameter Modification

It can be easily imagined that the influence of geometrical imperfections on the compressive response will be decreased as the designed strut diameter d increases under the assumption that all struts have the same scale of imperfections. In this study, additional three kinds of lattice

block specimens were prepared, and their included geometrical imperfections and compressive response were confirmed. Here, each specimen was designed with different strut diameters (d = 0.2, 0.4, and 0.5 mm) and strut lengths (L = 2.5, 5.0, and 6.25 mm). After observing geometrical imperfections on all specimens as described in Section 2.2, the unified model was prepared using these results, and numerical calculations were performed. Also, compression tests were conducted. Since all specimens were designed under the same strut slenderness ratio $d/L = 0.08$, the stress-strain curve can be compared directly.

3 RESULTS AND DISCUSSION

3.1 Statistical Analysis of Geometrical Imperfections

Figure 6(a,b) and (c,d) show variations of probability density for a major axis a, minor axis b and the offset of center-axis (X,Y) obtained from a XRM data for a strut. The parameters on the horizontal axis of each figure are shown as ratios to the strut diameter of the as-designed model. As can be found from these figures, these density distributions are remarkably close to the Gaussian distribution curve. The mean value ν and the standard deviations σ are shown in these figures. Also, these results shown in Figure 6(a,b) and (c,d) are used as a reference data when we prepare FE lattice block models include the simplified geometrical imperfections.

3.2 Numerical Results

3.2.1 Evaluation about the Role of Single Geometrical Imperfection

In this study, the radius deviation model, the center-axis offset model and the unified imperfection model are prepared for investigating the effect of geometrical imperfections on the compressive response. Figure 7 shows stress-strain curves for perfect and imperfect lattice models. The black line shows the response for the perfect lattice model. Also, the blue line shows the predicted response of the model by considering the center-axis offset. The purple line shows the response by considering the radius deviation, and the red dashed line shows the response by including both of these geometrical imperfections. These curves represent the response of one representative lattice model with imperfection distributions statistically similar to the built samples. A shaded domain is also included within which fall the results of all ten imperfect-geometry numerical analyses. This region describes the probability distribution of possible mechanical responses. A comparison of these curves reveals the following:

- There are mainly two types of geometrical imperfections: radius deviation and center-axis offset, both of which contribute to the degradation of mechanical properties. In particular, the radius deviation has a greaterimpact on the degradation. This is because the radius deviation is more significant than the center-axis offset in terms of the average values and the standard deviation of defects, as shown in Figure 6.

- The unified imperfection model with two defects results in a further degradation of mechanical properties compared to the single geometrical imperfection model. Also, the response of the FE model, which is a probability distribution based on the observed geometrical imperfections, falls within a certain statistical domain. This is useful for predicting mechanical properties.

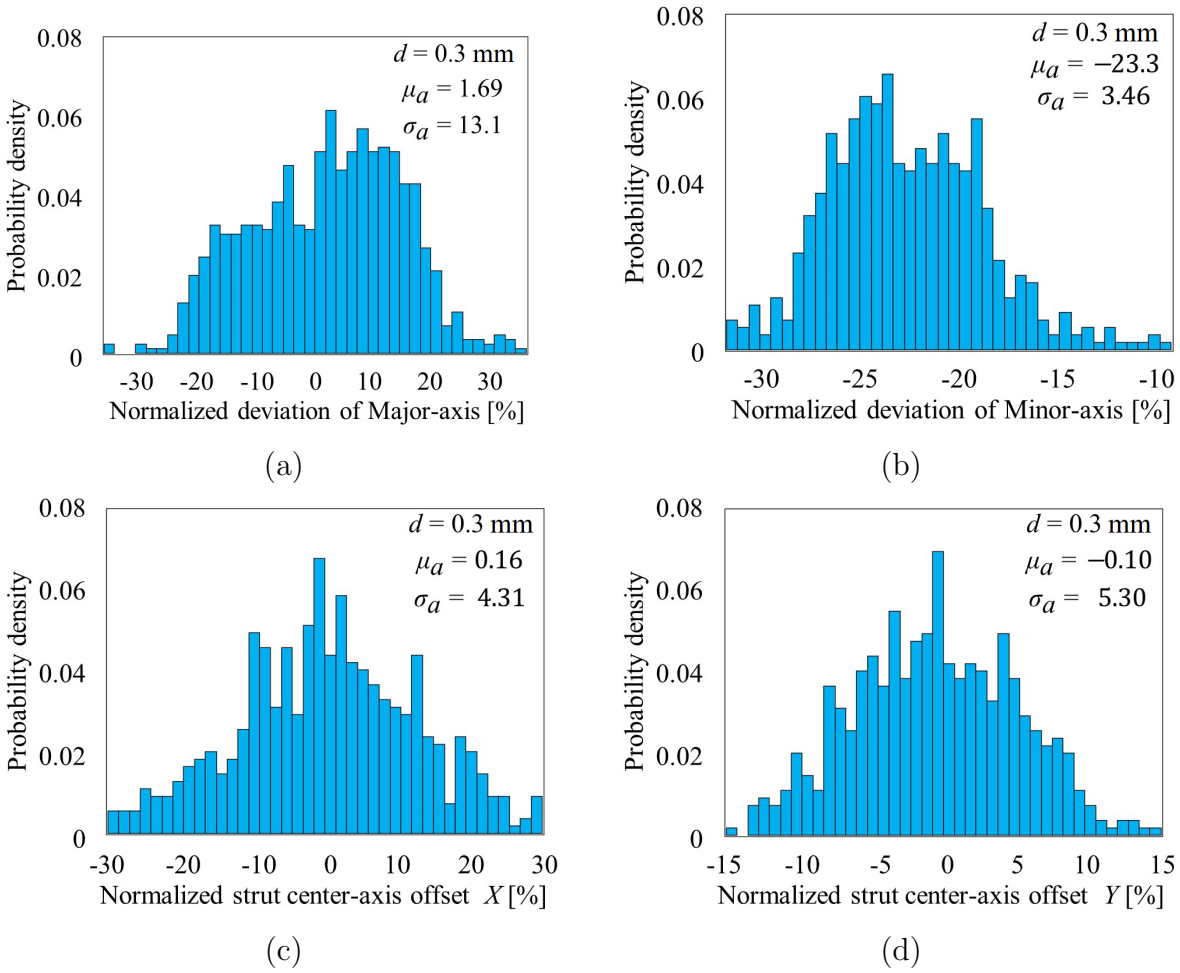

Figure 6: Imperfections in a lattice structure (d = 0.3 mm, L=3.75 mm)

3.2.2 Geometrical Imperfections Focused on Strut Diameter

In this section, we discuss the trend of geometrical imperfections observed in the lattice block fabricated with different strut diameters. The observed parameters are the major axis a, minor axis b, and the offset of the center-axis (X,Y). The variations of probability density for each parameter are shown in Figures 8(a,b) and 8(c,d). Since these density distributions were close to a Gaussian distribution curve, the average values ν and standard deviation σ were calculated and given the values in these Figures. The parameters on the horizontal axis of each figure are the same as in Figure 6. By comparing with these density distributions, the following points can be found:

- Regareding the radius deviation, when strut diameter was modified, minor axis was remarkably affected. For the specimens prepared in this study, average undersizing of 33.6 % occurred in the lattice block with the thinnest strut diameter (d = 0.2 mm).

- Regarding the center-axis offset, the average values were not much different among the models. However, the standard deviation showed a tendency for greater variability in models with smaller design diameters. When the designed strut diameter is thin, operating range of the fiber laser of the metal 3D printer is narrow, and the material powder

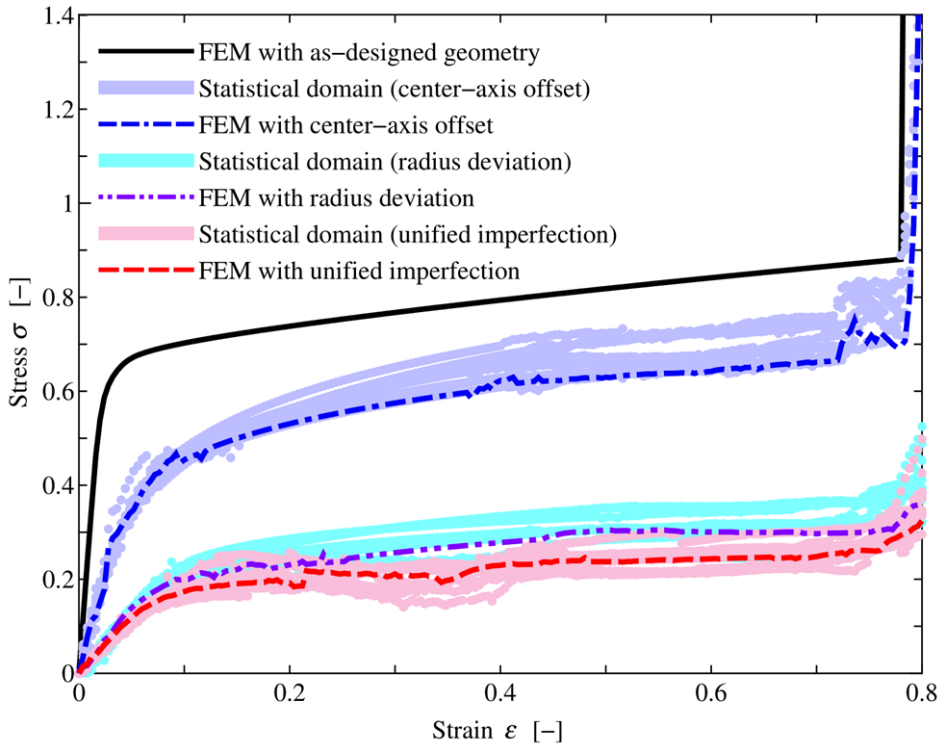

Figure 7: Stress-strain curve considering imperfection

cannot be melted efficiently. This may cause geometrical imperfections, which should be investigated further.

In section 3.2.1, it was confirmed that geometrical imperfections (radius deviation and center-axis offset) cause a degradation of mechanical properties. By considering these result, it is expected that the degradation of mechanical properties will be remarkable for the model with thin strut diameter.

3.2.3 Comparison between the FEM and Experiment Response

The experimental results of the compressive stress-strain curves for all lattice block specimens are shown in Figure 9. Also, numerical results of the FE model including the geometrical imperfections observed in Section 3.2.2 are shown in the same figure. The colors of the graph plots are the same as in Figure 8. The experimental results are plotted as triangles and the FEM curves as dashed lines. Based on the observed probability density of geometrical imperfections, ten kinds of FE models were prepared for each strut diameter. The response of one representative lattice model is shown in the graph. The black line shows the response for the as-designed model. All of the models in this study have the same strut slenderness ratio $d/L = 0.08$. Therefore, one as-designed curve can be compared to the curves of all specimens. Comparison of these curves reveals the following:

- It can be seen that as the strut diameter thick, the stress-strain curve approaches that of the design. Also, Figure 8 shows that geometrical imperfections (diameter deviation and

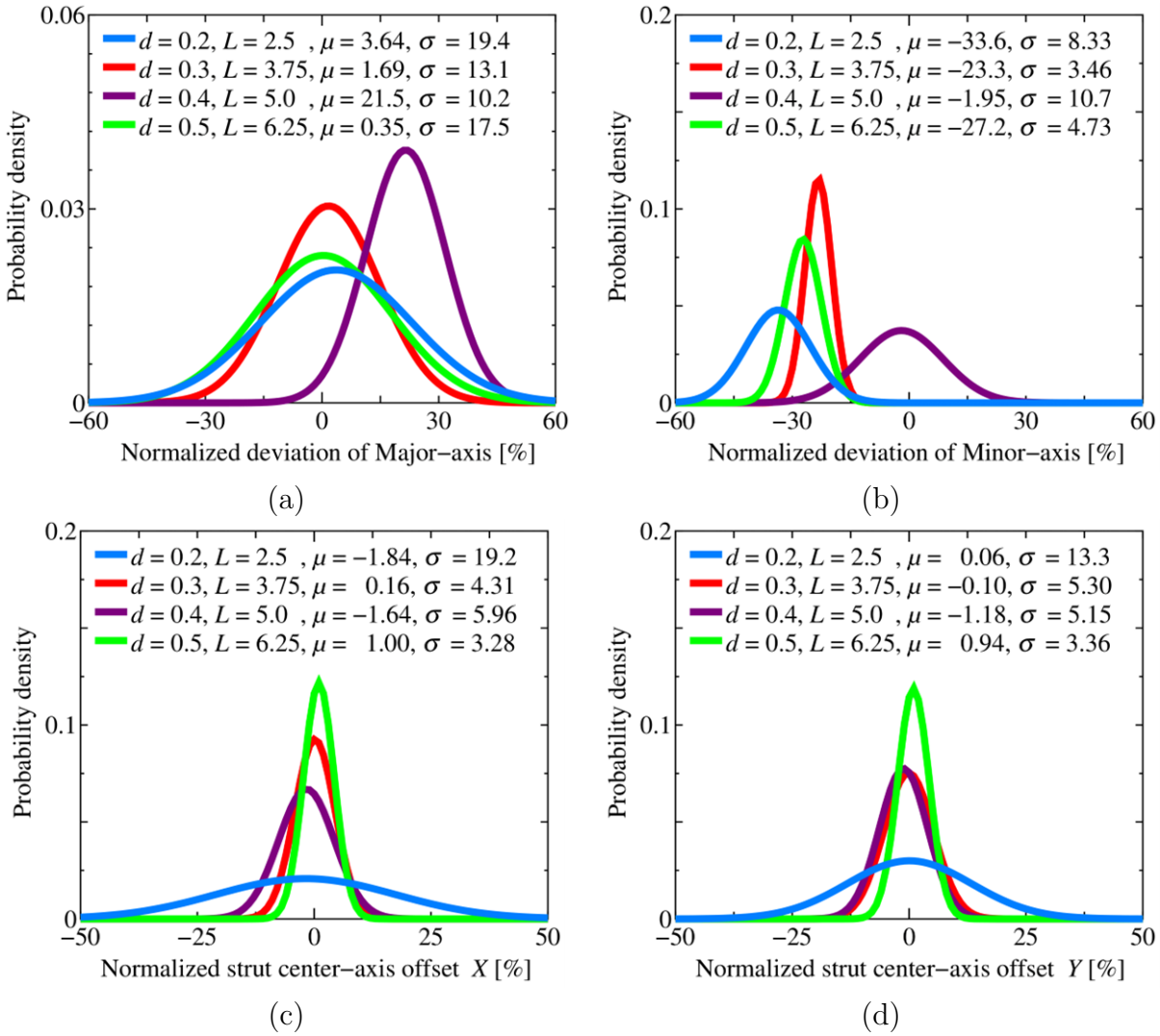

Figure 8: Geometric imperfections for different strut diameters

center-axis offset) are relatively smaller in the model with thick strut diameter. Based on these facts, it can be concluded that if the ratio of geometrical imperfections to the strut diameter can be lowered, the degradation of the mechanical properties can be limited.

- Numerical results for these FE models agree fairly well with the experimental result, which assures the effectiveness of our FE simulation. It can be referred to the possibility of predicting the compressive response and the degradation of mechanical properties by observing the probability distribution of geometrical imperfections. It can be concluded that the allowable minimum strut diameter is around 0.4 mm if a lattice block is fabricated under the manufacturing conditions of this study and the degradation of mechanical properties is allowed up to 50 %.

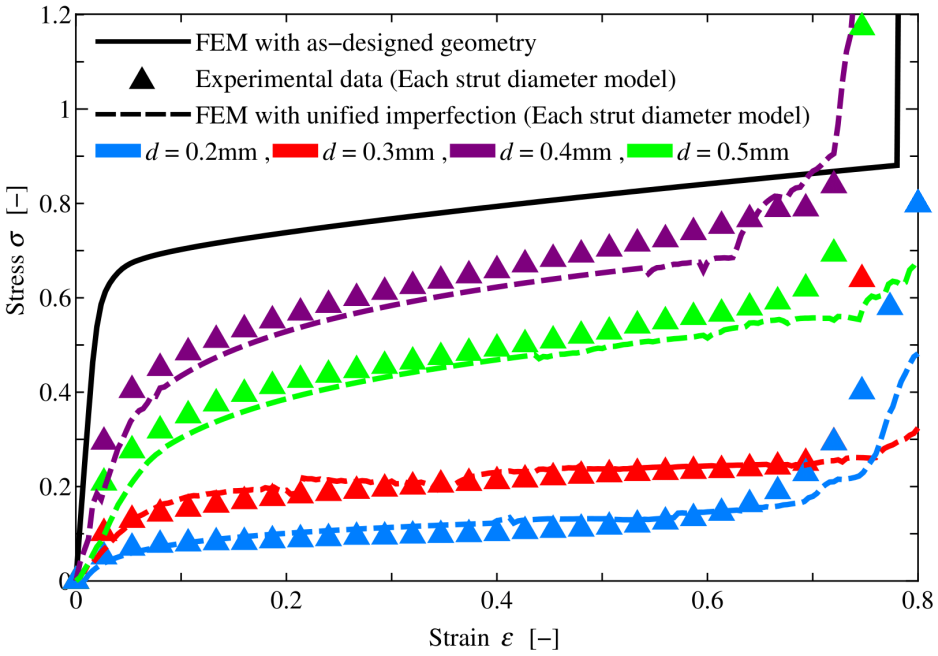

Figure 9: Stress-strain curve of Experiment and unified model

4 CONCLUSIONS

In this paper, the effects of geometrical imperfections existed in a lattice structure fabricated by metal 3D printer on the compressive response were investigated by using FE simulation. There are mainly two types of geometrical imperfections (strut diameter deviation and the center-axis offset), and the probability density distribution of them were measured. The compressive behaviour of a lattice block measured by experiment is close to a that for a FE model with imperfections. By reflecting these irregularities on our FE model, the degradation of mechanical properties from the idealized perfect FE model without imperfection can be fairly evaluated. Moreover, based on our FE simulation, the allowable minimum strut diameter for a BCC lattice was proposed in order to evaluate the compressive response without considering the geometrical imperfections.

REFERENCES

[1] Kyogoku, H. *Research Trend and Application of Additive Manufacturing*. Journal of smart processing, (2014) **3**: 148-151.

[2] Shimizu, T. and Kirihara, S. *Active contributions of additive manufacturing for sustainable development goals*. J Smart Processing, (2021) **10**: 152-158.

[3] Hanzl, P., Zetek, M., Bakša, T. and Kroupa, T. *The influence of processing parameters on the mechanical properties of SLM parts*. Procedia Engineering, (2015) **100**: 1405-1413.

[4] Cao, X., Jiang, Y., Zhao, T., Wang, P., Wang, Y., Chen, Z., et al. *Compression experiment and numerical evaluation on mechanical responses of the lattice structures with stochastic*

geometric defects originated from additive-manufacturing. Composites Part B: Engineering, (2020) **194**: 108030.

[5] Gumruk, R. and Mines, RAW. *Compressive behaviour of stainless steel micro-lattice structures*. Int J Mechanical Sci, (2013) **68**: 125-139.

[6] Liu, L., Kammc, P., García-Moreno, F., Banhart, J. and Pasini, D. *Elastic and failure response of imperfect three-dimensional metallic lattices: the role of geometric defects induced by selective laser melting*. J Mechanics and Physics of Solids, (2017) **107**: 160-184.

[7] Lozanovski, B., Leary, M., Tran, P., Shidid, D., Qian, M., Choong, P., et al. *Computational modelling of strut defects in SLM manufactured lattice structures*. Materials and Design, (2019) **171**: 107671.

[8] Frisch-Fay, R. *Flexible Bars*. Butterworths, (1962).